

# Lattice QCD for RHIC \*

SOURENDU GUPTA

Department of Theoretical Physics, Tata Institute of Fundamental Research,  
Homi Bhabha Road, Mumbai 400005, India.

I briefly introduce the methods by which lattice QCD predictions for RHIC are obtained. Next I deal with lattice determinations of strangeness production and event-to-event fluctuations of conserved quantities. I also present a new diagrammatic method for computing derivatives with respect to chemical potentials, and conclude with discussions of some tests of thermal perturbation theory which follow.

PACS numbers: 12.38.Gc, 12.38.Mh, 25.75.-q, 11.10.Wx, 11.15.Ha

## 1. Introduction

Heavy-ion collisions at the RHIC have already given evidence for dense and hot matter [1], and may lead to a discovery of the predicted plasma phase of QCD if such predictions are made precise enough. In recent years computations in lattice field theories have become precise enough to confront phenomenological analyses of experimental results. Among the many interesting results from RHIC [2] I single out three for comment— indications of early thermalisation leading possibly to hydrodynamic flow, rapid chemical saturation of strangeness, and fluctuations from one event to another. Each of these observations may be related to quantities which are easily computed in finite temperature lattice QCD. Flow is strongly connected to the equation of state, strangeness to the Wroblewski parameter, and fluctuations to various susceptibilities. The equation of state has been adequately dealt with elsewhere [3], and I will restrict myself to the rest.

Interesting thermodynamical quantities can be constructed by taking the derivative of the free energy with respect to intensive quantities. Consider QCD with the intensive variables temperature,  $T$ , and the quark chemical potentials,  $\mu_u$ ,  $\mu_d$ ,  $\mu_s$  (for flavours  $u$ ,  $d$  and  $s$  of quarks). The first derivative

---

\* Presented at the 42nd Cracow School of Theoretical Physics, Zakopane, Poland

of the free energy,  $F$ , with respect to one of the chemical potentials is the quark number—

$$\langle n_f \rangle = \frac{\partial}{\partial \mu_f} F(T, \mu_u, \mu_d, \mu_s) = \frac{\partial}{\partial \mu_f} \log Z(T, \mu_u, \mu_d, \mu_s), \quad (1)$$

where  $Z$  is the partition function. The second derivatives are called quark number susceptibilities [4]

$$\chi_{fg} = \frac{\partial^2}{\partial \mu_f \partial \mu_g} F(T, \mu_u, \mu_d, \mu_s) = \frac{\partial \langle n_g \rangle}{\partial \mu_f} = \frac{\partial \langle n_f \rangle}{\partial \mu_g}. \quad (2)$$

In general such second derivatives measure microscopic fluctuations in equilibrium. It has recently been discovered that these fluctuations,  $\chi_{fg}$ , may be directly accessible in heavy-ion collisions [5]. Higher derivatives, which we deal with later, may be called non-linear quark number susceptibilities, in analogy with similar quantities in condensed matter physics.

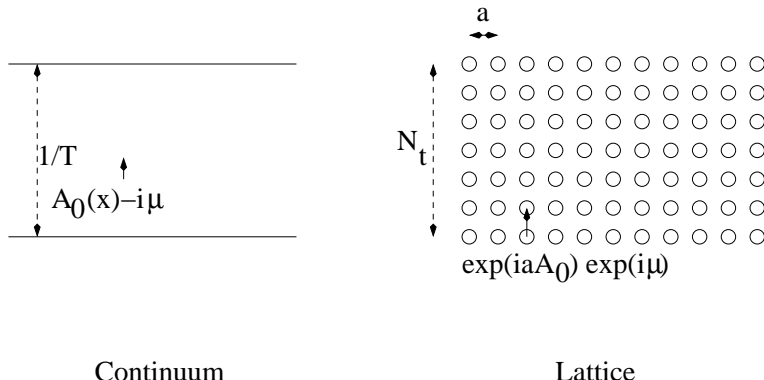


Fig. 1. Finite temperature Euclidean field theory in the continuum and on a lattice.

I will describe information on these derivatives which we have obtained from lattice simulations of QCD. These are numerical estimates of the QCD partition function,  $Z$ , in the Euclidean thermal field theory context—

$$Z(T, \mu_u, \mu_d, \mu_s) = \int dU \prod_{f=u,d,s} \det M(m_f, \mu_f) \exp[-S(U)]. \quad (3)$$

In this formula  $S(U)$  is the gauge part of the action,  $M$  is the Dirac operator for quarks of mass  $m_f$  with chemical potential  $\mu_f$ , and the integration is performed over all configurations of gauge fields. The chemical potentials enter the Dirac operator as if they were constant  $U(1)$  gauge fields (see

Figure 1). In the Euclidean formulation of finite temperature field theory the temperature enters indirectly through the fact that the Euclidean ‘time’ direction is of extent  $1/T$  [6].

Since such integrals have the usual ultraviolet divergences of field theory, they can be defined with a space-time lattice as a regulator. The spacing between lattice sites in all directions is  $a$ . The gauge field  $A_\mu$  associated with infinitesimal changes in position, *i.e.*,  $\partial_\mu$ , is replaced by the finite transporter  $\exp(iaA_\mu)$ . The number of lattice sites in the time direction is  $N_t$ . At fixed temperature this gives the relation

$$aN_t = 1/T, \quad (4)$$

This is used to eliminate the ultraviolet cutoff,  $\Lambda = 1/a$  from all computations in favour of the physical scale  $T$ . After this is done, the regulator must be removed by taking  $\Lambda \rightarrow \infty$  while holding fixed all physical quantities. This process is called “taking the continuum limit”, since it means that  $a \rightarrow 0$  at fixed temperature by taking  $N_t \rightarrow \infty$  while holding  $T$  constant (see Figure 1).

Taking the continuum limit is exactly the same as normalizing the field theory. A measurement of the renormalized strong coupling at the scale of  $1/a$  flows according to the two-loop  $\beta$ -function of QCD. As a result, good control over the continuum extrapolation comes from perturbation theory, yielding [7]

$$\frac{T_c}{\Lambda_{\overline{MS}}} = \begin{cases} 1.15 \pm 0.05 & (N_f = 0), \\ 0.49 \pm 0.05 & (N_f = 2). \end{cases} \quad (5)$$

This gives us good precision in pinning down the running coupling at any given temperature since  $\log(T/\Lambda_{\overline{MS}}) = \log(T/T_c) + \log(T_c/\Lambda_{\overline{MS}})$ .  $T_c/\Lambda_{\overline{MS}}$  is a reasonably easy quantity to measure because there are nice definitions of the renormalized QCD coupling on the lattice which show the usual logarithmic scaling without any power corrections in  $a$ . Other quantities may have power corrections which need to be subtracted before the logarithmic scaling can be seen. While this is tedious, the great advantage of the lattice is that it allows full control over infrared divergences which plague finite temperature field theory.

Another fact is crucial. In a lattice computation we do not determine the integral in eq. (3) before taking its derivatives. Instead, we take the derivatives before doing the integral numerically. For example, we notice that for any matrix  $M(x)$  where each matrix element may depend on some variable  $x$

$$\frac{\partial \det M(x)}{\partial x} = \det M(x) \text{Tr } M' M^{-1}, \quad (6)$$

where  $M'$  denotes the matrix each term of which is the derivative of the corresponding term of  $M$ . As a result,

$$\langle n_i \rangle = \frac{1}{Z} \int dU \text{Tr} M'_i M_i^{-1} \prod_f M_f \exp[-S(U)] = \langle \text{Tr} M'_i M_i^{-1} \rangle. \quad (7)$$

The expectation value on the right is computed with a Monte Carlo procedure which simulates the integrand of eq. (3) [8]. Such a procedure works only when the integrand is non-negative. Since the Euclidean Dirac operator with chemical potential has complex eigenvalues, the determinant is not positive definite, and lattice Monte Carlo simulations of QCD at finite chemical potential become tremendously hard to do. In all the work reported here we deal with the susceptibilities evaluated at zero chemical potential. Interestingly, they can be (and have been) used to continue lattice QCD information to non-zero chemical potential [9].

Finally a word about flavour symmetry breaking. If the  $u$  and  $d$  quark masses in nature were equal then flavour symmetry would be broken only in electro-weak interactions. Lattice QCD computations are done in this limit. In reality, however,  $u$  and  $d$  quark masses differ. It turns out that this breaking is almost irrelevant to thermodynamics [10]. The strange quark is much heavier, with a mass not much different from  $T_c$ . Hence it is almost quenched close to  $T_c$  but should be treated as unquenched far above  $T_c$ .

## 2. Fluctuations

### 2.1. Lattice Measurements

I will introduce some notation. The usual baryon chemical potential is  $\mu_0 = (\mu_u + \mu_d + \mu_s)/3$ . The chemical potential associated with the isospin quantum number is  $\mu_3 = (\mu_u - \mu_d)/2$ . The corresponding number densities are  $\langle n_0 \rangle = \langle n_u + n_d + n_s \rangle / 3$  and  $\langle n_3 \rangle = \langle n_u - n_d \rangle / 2$ . These are zero whenever the chemical potentials vanish. The susceptibilities obtained by taking double derivatives with respect to  $\mu_0$  and  $\mu_3$  are written  $\chi_0$  and  $\chi_3$ . These can be non-zero even when the chemical potentials vanish.

We recently improved upon previous measurements [4, 11] of these quantities in several ways. First, by changing the size of the spatial box within which the lattice computation is done, we have found a range of sizes such that the box has no effect on the physical measurement. All our subsequent measurements are in this range of box sizes. Secondly, unlike previous computations, we have held the quark mass,  $m$ , fixed in terms of physical mass scales such as GeV or  $T_c$  as we change the temperature. Previous studies had, for convenience, fixed  $ma = m/TN_t$ , which meant that their quark

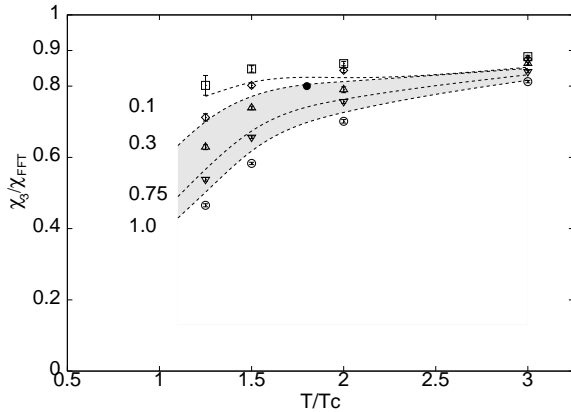


Fig. 2. The susceptibility  $\chi_3$  as a function of  $T$  for several different valence quark masses,  $m_v$  and lattice spacing  $a = 1/4T$ . The lines summarize data for quenched QCD while the symbols are for data in  $N_f = 2$  QCD for the  $m_v/T_c$  values shown. Error bars are mostly smaller than the symbols. The shaded region covers a range of quark masses appropriate to strange quarks.

mass changed as they scanned across temperature. Finally, by improving the estimators of the traces, it turns out that modern computers can allow us to reduce the error bars in some of the susceptibilities by over 3 orders of magnitude—an effective gain of a factor of a over million in the statistics available ten years ago when the last computations were performed.

For  $a = 1/4T$ , *i.e.*,  $N_t = 4$ , our simulations with the quenched theory ( $N_f = 0$ ) [12] and with two light flavours of sea quarks ( $N_f = 2$ ) [13] showed that the susceptibility is quite different from that for the ideal gas,  $\chi_{FFT}$ , on the same lattice. There is a small effect from unquenching the light sea quarks—about 5%. Since this effect is so small, it seems that the effect of unquenching the strange quark should be smaller than the statistical errors in our measurement. By making the valence quark heavier we can therefore investigate the dynamics of strange quarks. We will return to this important point later.

The quark mass dependence of  $\chi_3$  is quite nontrivial and is interesting in itself. It has been known for a long time that  $\chi_3$  can be written as the zero-momentum limit of a certain component of a vector correlation function at finite temperature [6]. Now, the breaking of Lorentz symmetry at finite temperature due to the selection of a preferred frame (that of the heat bath) means that angular momenta do not necessarily label the states of the system [15]. One of the most well-known consequences of this is the difference between electric and magnetic polarizations of gauge bosons

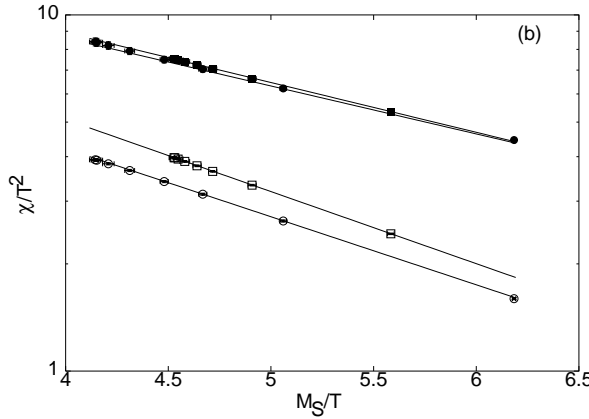


Fig. 3. The dependence of  $\chi_3$  and the pseudo-scalar susceptibility,  $\chi_\pi$ , on the common screening mass of the scalar and pseudo-scalar at  $T = 1.5T_c$  and  $2T_c$ . Error bars are smaller than the symbols.  $\chi_\pi$  is the zero-momentum pseudo-scalar correlator [14].

at finite temperature [16]. In any case, this broken symmetry causes  $\chi_3$  to mix with scalar/pseudo-scalar representations [17, 13]. Previous work on the lattice has seen clearly that correlations in this channel at high temperatures deviate strongly from that of an ideal quark gas [18]. As the quark mass is changed, this correlation function, the corresponding screening mass, and  $\chi_3$  all change in response (see Figure 3).

The flavour off-diagonal susceptibility  $\chi_{ud}$  turns out to be surprisingly small. Our measurements reveal that above  $T_c$  the dimensionless number  $\chi_{ud}/T^2$  is zero to within a few parts in  $10^5$ . This is a major surprise, because a recent computation in resummed finite temperature QCD shows that this quantity should be of the order of  $\alpha_s^3(2\pi T) \log \alpha_s(2\pi T)$  and predicts that it should be of order  $10^{-3}$  [19]. A non-log contribution of order  $\alpha^3(2\pi T)$  remains to be computed, but even if this cancels the computed term at some  $T$ , the range of temperatures over which results are available is large enough that a substantial non-zero value would still be seen. This disagreement between the lattice and perturbative computations stand as a puzzle.

Below  $T_c$  this off-diagonal susceptibility has only been investigated in the quenched theory. It is small but clearly non-zero (see Figure 4). With changing quark mass it is seen to vary roughly as  $1/m_\pi^2$  where  $m_\pi$  is the pion screening mass, showing that such fluctuations are essentially carried by pions. The connection between the vector-vector correlator  $\chi_{ud}$  and the

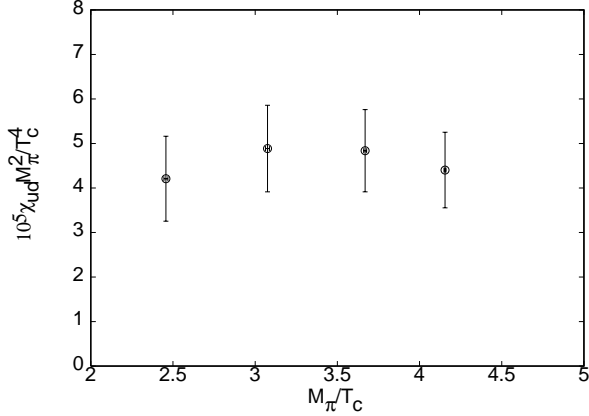


Fig. 4. The dependence of  $\chi_{ud}$  on  $m_\pi$  at  $T = 0.75T_c$  in quenched QCD.

pion below  $T_c$  comes from the fact that the contribution

$$\gamma_0^\tau \bullet \text{---} \circlearrowleft \pi \text{---} \circlearrowright \bullet \gamma_0^\tau \quad (8)$$

to  $\chi_{ud}$  is allowed at finite temperature, and therefore, dominates  $\rho$  exchange contributions purely kinematically. This is another manifestation of the same physics that led to the correlation shown in Figure 3. While  $\chi_{ud}$  is non vanishing below  $T_c$ ,  $\chi_3$  is consistent with zero.

Continuum extrapolation of these results have been attempted [20, 21, 22]. It turns out that  $\chi_3$  measured with staggered Fermions have large power corrections in  $a$ . As a result, the ratio  $\chi_3/\chi_{FFT}$  at  $T = 2T_c$  decreases from  $a = 1/4T$  to  $1/6T$  but then turns over and approaches the limit from below. The same limit is obtained by extrapolating  $\chi_3/T^2$  using the usual staggered Fermions or an improved version, although both these extrapolations approach the limit more smoothly. The results at  $2T_c$  are in marginal disagreement with the resummed perturbative computations of [19] (*i.e.*, disagrees at the  $1-\sigma$  level but agrees at  $3-\sigma$ ), but become compatible with it at  $T = 3T_c$ .  $\chi_{ud}/T^2$  remains compatible with zero at the level of a few parts in  $10^{-5}$  in the continuum limit.

## 2.2. Applications to phenomenology

Two important qualitative observations emerge from the lattice computation. First, that above  $T_c$  one has non-vanishing  $\chi_3$  but  $\chi_{ud}$  is zero. Second, that below  $T_c$   $\chi_3$  vanishes and  $\chi_{ud}$  is non-zero. Since there are only two independent types of susceptibilities (as I show later), all fluctuations

of interest are governed by these two and their changes with valence quark mass.

Fluctuations of electric charge, for example, are controlled by the susceptibility

$$\chi_q = \frac{1}{9} (10\chi_3 + \chi_s + \chi_{ud} - 2\chi_{us}), \quad (9)$$

whereas baryon number fluctuations are related to

$$\chi_0 = \frac{1}{9} (4\chi_3 + \chi_s + 4\chi_{ud} + 4\chi_{us}). \quad (10)$$

The following quantitative conclusions can be obtained—

1. For  $T \gg T_c$ , since  $\chi_3 \approx \chi_s \gg \chi_{ud} \approx \chi_{us}$ , we have  $\chi_q \approx (11/9)\chi_3$  and  $\chi_0 \approx (5/9)\chi_3$  so that the ratio  $\chi_q/\chi_0 \approx 2$ .
2. When  $T > T_c$  but very close to  $T_c$ , since  $\chi_3 \gg \chi_s \gg \chi_{ud} \approx \chi_{us}$ , we find  $\chi_q \approx (10/9)\chi_3$  and  $\chi_0 \approx (4/9)\chi_3$  so that the ratio  $\chi_q/\chi_0 \approx 2.5$ .
3. For  $T < T_c$  since  $\chi_{ud} \propto 1/m_\pi^2$  and assuming that  $\chi_{us} \propto 1/m_K^2$ , since  $\chi_3 \approx \chi_s \approx 0$ , we expect that  $\chi_q/\chi_0 \approx 0.25 + \mathcal{O}(m_\pi^2/m_K^2)$ .

Under the assumptions given above, there are diametrically opposite predictions above and below  $T_c$ —

$$\begin{aligned} \chi_0 &< \chi_q & & (T > T_c) \\ \chi_0 &> \chi_q & & (T < T_c) \end{aligned} \quad (11)$$

The ordering of fluctuations in baryon number [23], charge [5] and total strangeness [24] are therefore radically different above and below the phase transition.

### 3. Strangeness production

Strangeness abundances in heavy-ion collisions at the CERN SPS collider and the RHIC have been analyzed extensively. There is some consensus that the observed chemical composition is that in equilibrium close to  $T_c$ , and that it cannot arise due to hadronic rescatterings [25]. One of the central quantities that has been extracted from data is the Wroblewski parameter

$$\lambda_s = \frac{2\langle \bar{s}s \rangle}{\langle \bar{u}u \rangle + \langle \bar{d}d \rangle}. \quad (12)$$

The averages on the right are defined to be the number of primary created quark pairs of each flavour. It turns out that lattice determinations of static

equilibrium quantities can be used to predict this dynamical quantity under some well-defined, and testable, assumptions.

As a preparatory example, consider the electrons in a metal interacting with external fields. In a static magnetic field,  $H$ , at a fixed temperature, the response is an induced magnetization whose rate of change with the field strength is the magnetic susceptibility,  $\chi(0)$ . This is a measure of the fluctuations of spins in thermal equilibrium. On the other hand, when an electromagnetic wave of frequency  $\omega$  propagates through the medium, it is attenuated due to dissipative phenomena which generate many excitations in the medium. One can describe the dissipation through a complex susceptibility  $\chi(\omega)$ , describing the response of the material to a magnetic field,  $H(\omega)$  of frequency  $\omega$  [27]. Causality relates the real and imaginary parts of  $\chi(\omega)$  through a Kramers-Krönig dispersion relation. From the fluctuation-dissipation theorem it is possible to deduce that the complex susceptibilities are proportional to the static susceptibility if the characteristic time scales of the system are very different from the energy scales dominating the production process [28].

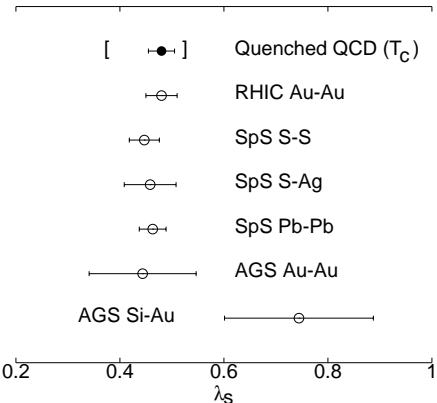


Fig. 5. The Wroblewski parameter on the lattice compared with extraction from data [26]. The error bars are statistical errors. For the lattice extraction the bracketed interval an estimate of possible errors due to extrapolation to  $T_c$ .

This carries over to strangeness production. The rate of production of quark pairs is proportional to a complex susceptibility, and hence to the static susceptibility that we measure. This gives

$$\lambda_s = \frac{2\chi_s}{\chi_u + \chi_d} = \frac{\chi_s}{\chi_u}, \quad (13)$$

where the susceptibilities are evaluated at the temperature and chemical

potential characteristic of the collision. In Figure 5 we display our prediction of  $\lambda_s$ , from the lattice computations already outlined, and a comparison with values extracted from experiments. Further details, including a complete list of all assumptions and ways to test them, can be found in [20].

#### 4. Testing perturbation theory

We have already seen evidence of non-perturbative effects in the susceptibilities. We extend this observation by investigating non-linear susceptibilities. We define these as higher derivatives of the free energy—

$$\chi_{fgh\dots} = \frac{\partial^n \log Z}{\partial \mu_f \partial \mu_g \partial \mu_h \dots}, \quad (14)$$

where the flavour indices  $f, g, h, \dots$ , need not be distinct. There is a nice and systematic way of evaluating the derivatives of  $Z$ . It begins by noting that the chemical potentials  $\mu_f$  appear in the partition function of eq. (3) only through the quark determinant. Then, we can evaluate the derivatives at by a chain rule starting with

$$\frac{\partial \det M}{\partial \mu_f} = \det M \mathcal{O}_f^{(1)}, \quad \frac{\partial^2 \det M}{\partial \mu_f \partial \mu_g} = \det M \left[ \mathcal{O}_f^{(1)} \mathcal{O}_g^{(1)} + \delta_{fg} \mathcal{O}_f^{(2)} \right], \quad (15)$$

etc. The operators  $\mathcal{O}_f^{(n)}$  are defined recursively through the relations

$$\mathcal{O}_f^{(n)} = \frac{\partial \mathcal{O}_f^{(n-1)}}{\partial \mu_f}, \quad (16)$$

and the concrete computational rules are—

$$\mathcal{O}_f^{(1)} = \text{Tr } M_f' M_f^{-1}, \quad \frac{\partial M_f^{-1}}{\partial \mu_f} = -M_f^{-1} M_f' M_f^{-1}. \quad (17)$$

This is the complete set of rules for writing down the operator expressions for the non-linear susceptibilities [29].

In the continuum theory, since the Dirac operator contains  $\mu$  linearly, second and higher derivatives,  $M_f''$  etc., vanish. Every  $M_f'$  corresponds to an insertion of  $\gamma_0 \lambda_f$  (where  $\lambda_f$  is a flavour generator) [30], and each  $M_f^{-1}$  is a quark propagator. Thus the chain rule (eqs. 15–17) can be written diagrammatically. The rules for a susceptibility of order  $n$  are—

1. Put down  $n$  blobs (each corresponding to an  $M_f'$ , i.e., a derivative with respect to  $\mu_f$ ) and label each with its flavour index.

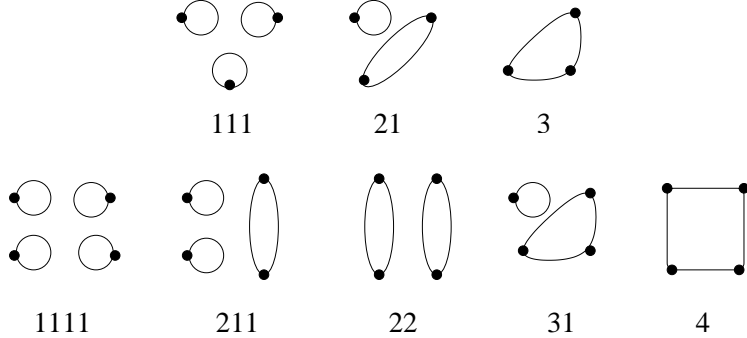


Fig. 6. The operator topologies which contribute to the third and fourth order susceptibilities.

2. Join the blobs by lines (each representing an  $M_f^{-1}$ ) into sets of closed loops such that each loop contains only blobs of a single flavour. Count the number of ways in which each topology arises and sum them all up.
3. For degenerate flavours for  $\mu_f = 0$ , the operator depends only on the topology and the flavour label on  $\mathcal{O}_f^{(n)}$  is irrelevant. So delete all the flavour indices after the counting is done.
4. The operators can then be labeled only by the topology, which is specified completely by the number of blobs per loop and the number of such loops. Thus, each distinct topology is a partition of  $n$ .

In Figure 6 are shown the topologies that contribute to the 3rd and 4th order susceptibilities. There are clearly two types of operators—one quark line connected operator for each  $n$ , and the remaining quark line disconnected. Flavour off-diagonal operators are necessarily quark-line disconnected. Since the free energy is even in each  $\mu_f$ , the odd-order susceptibilities vanish for  $\mu = 0$ , just as do the number densities.

The rules show that  $V\chi_{uu}/T = \langle \mathcal{O}_2 + \mathcal{O}_{11} \rangle$  and  $V\chi_{uud}/T = \langle \mathcal{O}_{11} \rangle$ . Due to flavour symmetry,  $\chi_{uu} = \chi_{dd}$ . The number of independent physical quantities, *i.e.*, susceptibilities, is equal to the number of operators. Hence, the operator expectation values are themselves physical. At third order  $V\chi_{uud}/T = \langle \mathcal{O}_{111} + \mathcal{O}_{12} \rangle$  and  $V\chi_{uuu}/T = \langle \mathcal{O}_{111} + 3\mathcal{O}_{12} + \mathcal{O}_3 \rangle$ . Flavour symmetry gives two different physical quantities— $\chi_{uuu} = \chi_{ddd}$  and  $\chi_{uud} = \chi_{udd}$  whereas there are three different operators. At fourth order, there are three different physical quantities, which are  $\chi_{uuuu} = \chi_{dddd}$ ,  $\chi_{uuud} = \chi_{uudd}$  and  $\chi_{uudd}$ , but five different operators. Due to flavour symmetry, the

number of different  $n$ -th order susceptibilities is equal to  $1 + n/2$  for even  $n$  and  $(1 + n)/2$  for odd  $n$ , whereas the number of distinct matrix elements is the number of partitions of  $n$ . For  $n > 2$  there are more matrix elements than susceptibilities, and the former cannot all be physical. The particular fourth order susceptibility—

$$\chi_{uudd} = \frac{T}{V} \langle \mathcal{O}_{1111} + 2\mathcal{O}_{211} + \mathcal{O}_{22} \rangle - \chi_{uu}^2 - 2\chi_{ud}^2 \quad (18)$$

is a cumulant related to the Binder variable [32] and hence interesting to study.

For each  $n$  only one of the susceptibilities, that with only a single flavour, contains a quark-line connected diagram. All other susceptibilities are necessarily quark-line disconnected. We have investigated some of these quark-line disconnected quantities numerically. In dynamical QCD with  $N_f = 2$  at temperatures  $T \geq 1.5T_c$ , it turns out that  $\chi_{ud}/T^2$  vanishes to one part in  $10^5$ , and both  $\chi_{uud}/T^3$  and  $\chi_{uudd}/T^4$  vanish to better than one part in  $10^3$ .

While the quark-line disconnected diagrams are expected to vanish in an ideal gas, in QCD they may be connected by gluon lines, and dressed by all possible gluon and quark loops. In [19] certain power counting rules were developed which may be applied to operators such as these: the main ingredient being that every loop with  $n$  blobs connects to  $n_g$  electric gluon lines, where  $n_g > 1$  and  $n_g + n$  is even. As a result,  $\langle \mathcal{O}_{11} \rangle \propto g^6$  (actually  $g^6 \ln g$  as shown in [19] after a detailed computation). All contributions to the third order susceptibility vanish. Of the diagrams contributing to  $\chi_{uudd}$ ,  $\langle \mathcal{O}_{22} \rangle \propto g^4$  and gives the leading perturbative contribution. At temperatures of  $2T_c$ , for  $N_f = 2$ , we get  $\langle \mathcal{O}_{11} \rangle/T^2 \approx 0.1$ , and  $\chi_{uudd}/T^4 \approx 0.5$ . These rough perturbative estimates can easily be modified by an order of magnitude due to subleading logarithms and numerical coefficients. Nevertheless, the lattice results are significantly below the perturbative estimates, and temperature independent over a range of temperatures where the perturbative estimates vary by a factor of 5.

This finite temperature analogue of Zweig's rule holds in a region of temperatures away from  $T_c$ . Closer to  $T_c$  there is some evidence for non-zero values of  $\chi_{ud}$  [4, 11, 21] as well as  $\chi_{uudd}$ . Since these quantities measure departures from ideal gas behaviour, they would be very interesting quantities to study in the vicinity of the critical point of QCD.

It is a pleasure to thank the organizers for a wonderful school. I would also like to thank Jean-Paul Blaizot and my collaborators, Rajiv Gavai and Pushan Majumdar, for discussions.

## REFERENCES

- [1] L. McLerran, Invited talk at the ICQAQGP 2001, Jaipur, India, hep-ph/0202025; H. Satz, Opening talk at Quark Matter 2002, Nantes, France, hep-ph/0209181.
- [2] See <http://www.bnl.gov/RHIC/> for all recent results from the experiments at RHIC.
- [3] K. Kanaya, talk given at the Quark Matter 2002 meeting, Nantes, France, hep-ph/0209116.
- [4] S. Gottlieb *et al.*, *Phys. Rev. Lett.*, 59 (1987) 2247.
- [5] M. Asakawa, U. W. Heinz and B. Müller *Phys. Rev. Lett.*, 85 (2000) 2072; S. Jeon and V. Koch *Phys. Rev. Lett.*, 85 (2000) 2076; see also the talk by V. Koch in these proceedings.
- [6] J. I. Kapusta, *Finite Temperature Field Theory*, Cambridge University Press, 1989.
- [7] S. Gupta, *Phys. Rev. D* 64 (2001) 034507.
- [8] Notice that two conceptually different quark masses appear in eq. (7). The valence quark mass,  $m_v$ , appears in the operator whose expectation value is measured—the trace in this case. The sea quark mass,  $m$ , appears in the measure, *i.e.*, the determinants.
- [9] Z. Fodor and S. D. Katz, *J. High Energy Phys.*, 03 (2002) 014; C. R. Allton *et al.*, hep-lat/0204010; P. de Forcrand and O. Philipsen, hep-lat/0205016; M. D'Elia and M.-P. Lombardo, hep-lat/0205022.
- [10] R. V. Gavai and S. Gupta, hep-lat/0208019.
- [11] R. V. Gavai *et al.*, *Phys. Rev. D* 40 (1989) 2743; C. Bernard *et al.*, *Phys. Rev. D* 54 (1996) 4585; S. Gottlieb *et al.*, *Phys. Rev. D* 55 (1997) 6852.
- [12] R. V. Gavai and S. Gupta, *Phys. Rev. D* 64 (2001) 074506.
- [13] R. V. Gavai, S. Gupta and P. Majumdar, *Phys. Rev. D* 65 (2002) 054506.
- [14] S. Gupta, *Phys. Lett.*, B 288 (1992) 171; G. Boyd *et al.*, *Z. Phys.*, 64 (1994) 331.
- [15] B. Grossman *et al.*, *Nucl. Phys.*, B 417 (1994) 289; P. Arnold and L. G. Yaffe, *Phys. Rev.*, D 49 (1994) 3003; S. Datta and S. Gupta, *Nucl. Phys.*, B 534 (1998) 392.
- [16] H. A. Weldon, *Phys. Rev.*, D 26 (1982) 1394.
- [17] S. Gupta, *Phys. Rev. D* 60 (1999) 094505.
- [18] C. DeTar and J. B. Kogut, *Phys. Rev. Lett.*, 59 (1987) 399; A. Gocksch *et al.*, *Phys. Lett.*, B 205 (1988) 334; K. D. Born *et al.*, *Phys. Rev. Lett.*, 67 (1991) 302; T. Hashimoto *et al.*, *Nucl. Phys.*, B 400 (1993) 267; P. de Forcrand *et al.*, *Phys. Rev.*, D 63 (2001) 054501; R. V. Gavai *et al.*, *Phys. Rev. D* 65 (2002) 094504; E. Laermann and P. Schmidt, *Eur. Phys. J.*, C 20 (2001) 541.
- [19] J.-P. Blaizot, E. Iancu and A. Rebhan, *Phys. Lett.*, B 523 (2001) 143, and hep-ph/0206280.

- [20] R. V. Gavai and S. Gupta, *Phys. Rev.*, D 65 (2002) 094515.
- [21] C. Bernard *et al.*, hep-lat/0209079.
- [22] R. V. Gavai and S. Gupta, in preparation.
- [23] Zi-Wei Lin and C. M. Ko, *Phys. Rev.*, C 64 (2001) 041901; D. Bower and S. Gavin, *Phys. Rev.*, C 64 (2001) 051902.
- [24] S. Jeon *et al.*, *Nucl. Phys.*, A 697 (2002) 546; M. Abdel-Aziz and S. Gavin, nucl-th/0209019.
- [25] P. Braun-Munzinger *et al.*, *Phys. Lett.*, B 465 (1999) 43; J. Letessier and J. Rafelski, *Nucl. Phys.*, A 661 (1999) 97c; F. Becattini *et al.*, *Phys. Rev.*, C 64 (2001) 024901; U. Heinz, *J. Phys.*, G 25 (1999) 263; R. Stock, *Phys. Lett.*, B 456 (1999) 277.
- [26] J. Cleymans, hep-ph/0201142.
- [27] Kapusta's computation of  $\chi_q$  as the self-energy of a photon propagating in the plasma [6], is precisely the static ( $\omega \rightarrow 0$ ) limit computation.
- [28] P. C. Martin in *Many Body Physics*, Proceedings of the 1967 Les Houches School, Eds. C. DeWitt and R. Balian, Gordon and Breach, New York, 1968; W. Marshall and S. W. Lovesey, *Theory of Thermal Neutron Scattering*, Oxford University Press, London, 1971; A. L. Fetter and J. D. Walecka, *Quantum Theory of Many-particle Systems*, McGraw-Hill, New York, 1971.
- [29] Similar expansions and diagrammatic rules can also be written for other quantities, such as the chiral condensate,  $\langle \bar{\psi} \psi \rangle = \text{Tr } M^{-1}$ , and hadron propagators.
- [30] The non-linear terms in  $\mu_f$  on the lattice are needed only for divergence cancellation (see [31]), and have no effect on the physics in the subsequent discussion.
- [31] R. V. Gavai, *Phys. Rev.*, D 32 (1985) 519.
- [32] A. Billoire *et al.*, *Phys. Rev.*, B 42 (1990) 6743; K. Binder *et al.*, *Phys. Rev.*, B 34 (1986) 1841.